Characterization of As-polluted soils by laboratory X-ray-based techniques coupled with sequential extractions and electron microscopy: the case of Crocette gold mine in the Monte Rosa mining district (Italy)

Ignazio Allegretta, Carlo Porfido, Maria Martin, Elisabetta Barberis, Roberto Terzano, et al.

Environmental Science and Pollution Research

ISSN 0944-1344
Volume 25
Number 25

Environ Sci Pollut Res (2018)
25:25080-25090
DOI 10.1007/s11356-018-2526-9

Springer

Environmental Science and Pollution Research (2018) 25:25080–25090
https://doi.org/10.1007/s11356-018-2526-9

RESEARCH ARTICLE

Characterization of As-polluted soils by laboratory X-ray-based techniques coupled with sequential extractions and electron microscopy: the case of Crocette gold mine in the Monte Rosa mining district (Italy)

Ignazio Allegretta[1] · Carlo Porfido[1] · Maria Martin[2] · Elisabetta Barberis[2] · Roberto Terzano[1] · Matteo Spagnuolo[1]

Received: 8 February 2018 / Accepted: 10 June 2018 / Published online: 24 June 2018

Abstract

Arsenic concentration and distribution were studied by combining laboratory X-ray-based techniques (wavelength dispersive X-ray fluorescence (WDXRF), micro X-ray fluorescence (μXRF), and X-ray powder diffraction (XRPD)), field emission scanning electron microscopy equipped with microanalysis (FE-SEM-EDX), and sequential extraction procedure (SEP) coupled to total reflection X-ray fluorescence (TXRF) analysis. This approach was applied to three contaminated soils and one mine tailing collected near the gold extraction plant at the Crocette gold mine (Macugnaga, VB) in the Monte Rosa mining district (Piedmont, Italy). Arsenic (As) concentration, measured with WDXRF, ranged from 145 to 40,200 mg/kg. XRPD analysis evidenced the presence of jarosite and the absence of any As-bearing mineral, suggesting a high weathering grade and strong oxidative conditions. However, small domains of Fe arsenate were identified by combining μXRF with FE-SEM-EDX. SEP results revealed that As was mainly associated to amorphous Fe oxides/hydroxides or hydroxysulfates (50–80%) and the combination of XRPD and FE-SEM-EDX suggested that this phase could be attributed to schwertmannite. On the basis of the reported results, As is scarcely mobile, even if a consistent As fraction (1–3 g As/kg of soil) is still potentially mobilizable. In general, the proposed combination of laboratory X-ray techniques could be successfully employed to unravel environmental issues related to metal(loid) pollution in soil and sediments.

Keywords Arsenic · Soil · Gold mine · X-ray microanalysis · Sequential extraction · SEM

Introduction

Arsenic (As) is a natural constituent of the earth crust and occurs at a concentration of 0.1–500 mg/kg in relation to the rock or soil genesis (Mandal and Suzuki 2002). However, in some cases, it can reach very high concentration levels due to industrial or mining activities (Vaughan 2006). Chronic exposure by ingestion of As is dangerous for human and animal health (Eisler 2004; Hopenhayn 2006). Therefore, restrictions have been imposed for total As concentration in water and soils (Decree of the Italian Ministry Council 2006; World Health Organization (WHO) 2011). In the last years, particular attention has been paid to the assessment of As bioavailability (Allegretta et al. 2017; Kim et al. 2014; Niazi et al. 2011; Porfido et al. 2016), since it is known that total As concentration does not reflect the real potential risk of the element, which is strictly related to its chemical forms. Among these, arsenate and arsenite species, for example, in the form of secondary As-bearing minerals (i.e., scorodite, arsenolite, and claudetite), are usually the oxidation products of primary minerals like arsenopyrite, orpiment, and realgar (Drahota and Filippi 2009). Arsenic mobility is strictly dependent on pH and redox conditions (Masscheleyn et al. 1991; Smedley and Kinninburgh 2002; Zobrist et al. 2000), but other parameters such as the soil chemical and mineralogical

Responsible editor: Philippe Garrigues

✉ Ignazio Allegretta
ignazio.allegretta@uniba.it

[1] Dipartimento di Scienze del Suolo, della Pianta e degli Alimenti, Università degli Studi di Bari "Aldo Moro", Via G. Amendola 165/A, 70126 Bari, Italy

[2] Dipartimento di Scienze Agrarie, Forestali e Alimentari, Università degli Studi di Torino, Largo Paolo Braccini 2, Grugliasco, 10095 Torino, Italy

composition (Lenoble et al. 2002; Violante and Pigna 2002) and the microbial activity (Fendorf et al. 2008; Lloyd and Oremland 2006) can influence it as well. Due to the complexity and heterogeneity of the soil system, a correct characterization and mobility assessment of As can be done only using a multianalytical approach (Haffert and Craw 2008; Kocourková-Višková et al. 2015; Lu and Zang 2005; Marabottini et al. 2013). X-ray-based analytical techniques have proved to be useful tools for the investigation of polluted soils. In particular, X-ray fluorescence spectroscopy (XRF) is a fast, non-destructive, and reliable technique for the determination of As concentration (Parson et al. 2013; Radu and Diamond 2009). X-ray diffraction (XRD) is widely used to study the mineralogical composition of soils. X-ray absorption spectroscopy (XAS) or X-ray photoelectron spectroscopy (XPS) can also provide more precise information about As minerals or As oxidation states (Arčon et al. 2005; Drahota et al. 2009; Javed et al. 2014; Kim et al. 2013; Lumsdone et al. 2001; Savage et al. 2000; Strawn et al. 2002). Finally, micro X-ray fluorescence (μXRF) and scanning electron microscopy coupled with energy dispersive X-ray fluorescence spectroscopy (SEM-EDX) are powerful tools to image the element distribution in the sample and its microstructure (Haffert and Craw 2008; Strawn et al. 2002).

In a number of studies dealing with As speciation in soil, synchrotron X-ray-based techniques have been adopted. However, this approach is not easily applicable, since synchrotron facilities are not promptly accessible to most scientists.

Although X-ray laboratory instruments cannot directly assess As speciation and mobility, they are often used to predict it, especially when complemented with sequential extraction procedures (SEP) (Drahota et al. 2009; Javed et al. 2014; Kim et al. 2014; Lu and Zang 2005).

Among anthropic activities, gold mining is the first responsible of As soil pollution (Eisler 2004). This is because gold lodes are usually associated with As sulfides (in particular, arsenopyrite), which are commonly treated as a waste and disposed of in the mining area (Morin and Calas 2006).

An important gold mining industry has been recorded in the Monte Rosa gold district (Piedmont, Italy). A number of mines are present in this area and the extracted materials were treated in the plants of Crocette, Pestarena, Guia, and Campioli-Lavanchetto (Caviglia et al. 2015). Despite these mines have been dismissed since the 1960s, and mine tailings are visible in several areas, only few studies have been published on the As contamination of the mining area. In particular, Marabottini et al. (2013) and Stazi et al. (2017) studied the As soil contamination around Pestarena mine. This site is of particular interest because of the very high As concentrations measured in some hotspots and the relatively scarce As mobility observed. Apart from the above-mentioned studies, no other work dealing with these sites has been published and, in particular, no data are available for the gold mine of Crocette. The understanding of the actual concentrations, distribution, and mobility of As would be of great help for the management and recovery of this gold mine and to understand the evolution and the risks associated with abandoned mining sites where tailings with high As content are disposed in forest environments.

In the present work, a multianalytical approach by combining laboratory X-ray-based techniques, field emission scanning electron microscopy coupled with microanalysis (FE-SEM-EDX), and a sequential extraction procedure was used to characterize As-polluted soils and determine As distribution as well as the mechanisms controlling its mobility and potential bioavailability. This type of information is of paramount relevance in environmental risk studies and cannot be obtained by simple standard analytical procedures. As a case study, three soils and a mine tailing, sampled around the abandoned gold mining site of Crocette (Monte Rosa, Piedmont, Italy), were investigated. In addition, a new hyperspectral XRF data analysis method, usually employed for cultural heritage studies (Van der Snickt et al. 2016), was used for the first time on environmental samples.

The multianalytical approach presented in this study aims at understanding the evolution and the risks associated to As in abandoned mining sites which can still endanger the surrounding environment.

Materials and methods

Sampling and preliminary analyses

Three soils and one mine tailing were collected near the former gold extraction plant located at Crocette (1400 m a.s.l.), along the Quarazza creek, a river flowing in a small lateral valley on the right side of the Anzasca valley (Macugnaga, Piedmont, Italy) (Fig. 1). The plant, established in 1936, was definitively closed in 1953. The plant, as well as some dumped mine tailings and flotation sediments, are located on a steep slope on the left side of the creek, mostly occupied by regosols and leptosols developing on metamorphic and igneous rocks of the Western Italian Alps (Costantini and Dazzi 2013). Forest trees and herbaceous vegetation are almost completely covering the site. No data about As pollution are available in the literature for this specific site.

In order to collect As-bearing samples, the element concentration was estimated in situ by a NITON XL3t 900 portable energy dispersive X-ray fluorescence (ED-XRF) spectrometer (Thermo Scientific) equipped with a Ag target (40 kV, 50 μA). Three different soils (S1, S2, and S3) and one mine tailing

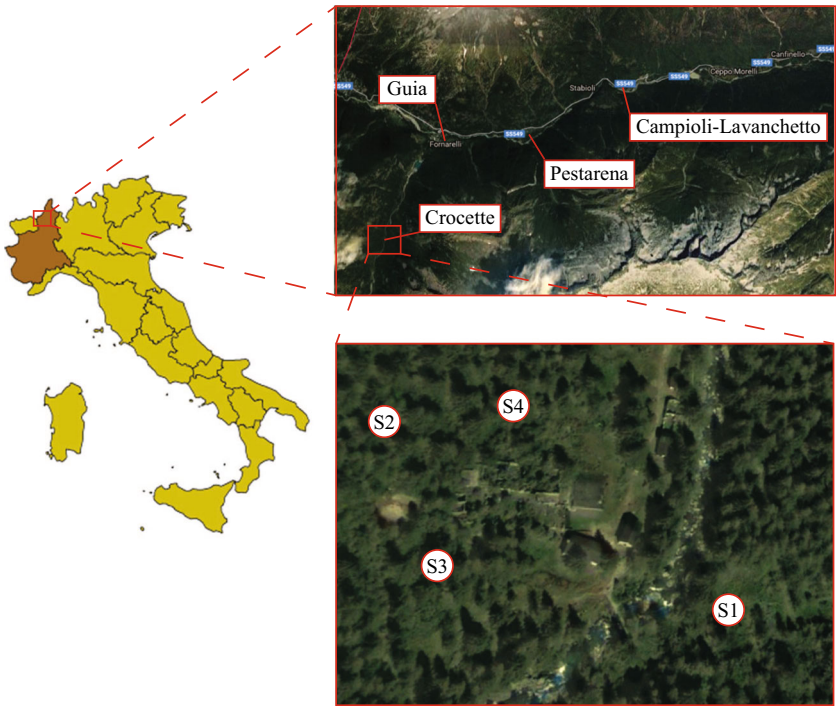

Fig. 1 Map of the Crocette mining area and identification of the sampling points S1, S2, S3, and S4

(S4) were chosen for their different As content. The S1 soil was collected on the right side of the creek (much less affected by the activity of the plant than the left side) and was used as control sample. Soils S2 and S3, as well as the mine tailings, were collected around the plant within a radius of 50 m. After removing the organic undecomposed litter, the first 15–20 cm of soil (roughly corresponding to the A soil horizon) were sampled. Six samples per soil and tailing were collected, stored in plastic containers (1 l) and then air dried in the laboratory. For each soil, the six samples collected were mixed together, sieved to 2 mm, and finally quartered. Soil physicochemical and mineralogical characterization were carried out on the quartered samples.

Physicochemical and mineralogical characterizations

Soil texture was determined using the pipette method (Indorante et al. 1990); pH was measured in double-distilled water; and total organic carbon (TOC) content was determined using the Walkley-Black method (Sparks 1996).

Major elements (Si, Al, Na, Mg, Ca, K, Ti, Mn, Fe, S, and P) and As concentration were determined by wavelength dispersive X-ray fluorescence (WDXRF) using a Supermini200 (Rigaku Corporation, Tokyo, Japan) spectrometer equipped with a Pd X-ray tube (50 kV, 4 mA) operating under vacuum (< 12 Pa). The calibration of the instrument and method validation were done using a series of geological standards provided by Service d'Analyses des Roches et des Minéraux (SARM, CRPG-CNRS, Vandoeuvre-les-Nancy, France). Five grams of quartered soil was manually ground in an agate mortar and mixed with 2 ml of a 15% (*w*/*w*) Elvacite® 2046 resin/acetone solution (PanAnalytical). After drying, the powder was poured into aluminum cups and pressed into pellets (4 tons/cm^2).

Mineralogical analyses were performed by X-ray powder diffraction (XRPD) using a Miniflex II (Rigaku Corporation, Tokyo, Japan) X-ray diffractometer equipped with a Cu tube (Cu Kα, 30 kV, 15 mA). Data were acquired between 3 and 70° 2θ with a step width of 0.02° 2θ and a counting time of 3 s/step. The incident beam passed through a 0.3-mm Soller slit, 1.25° divergent slit, a 10-mm mask, and emerged after a 1.25° antiscatter slit.

Sequential extraction procedure

A five-step SEP (Wenzel et al. 2001) was used to assess the potential mobility of As in the studied soils. The As forms extracted by SEP at different steps are:

1. *Non-specifically adsorbed,* extracted with $(NH_4)_2SO_4$ 0.5 M for 4 h at 20 °C;
2. *Specifically sorbed on minerals,* extracted with $NH_4H_2PO_4$ 0.5 M for 16 h at 20 °C;
3. *Associated to amorphous and scarcely ordered Fe and Al oxides and hydroxides,* extracted with NH_4-oxalate 0.2 M for 4 h at 20 °C;
4. *Associated to well-crystallized Fe and Al oxides and hydroxides,* extracted with NH_4-oxalate 0.2 M and ascorbic acid 0.1 M for 30 min at 96 °C;

5. *Residual,* extracted using acid microwave-assisted digestion with HNO_3 and H_2O_2 (7:1, *v*/*v*).

After each extraction step, the suspension was centrifuged for 15 min at 1700×*g* and the supernatant was filtered through 0.45 μm cellulose acetate filters. Arsenic concentration in the extracts was quantified by total reflection X-ray fluorescence spectroscopy (TXRF) using a S2 Picofox spectrometer (Bruker Nano GmbH, Berlin, Germany) equipped with a Mo target (50 kV, 600 μA), a multilayer monochromator, and a XFlash® silicon drift detector (energy resolution < 150 eV at 5 kcps at Mn Kα). In order to quantify As, 10 μl of Ga (100 mg/l) were added to 1 ml of the filtered extract as internal standard. After vortexing, 10 μl of solution were pipetted onto a quartz carrier and dried on a hot plate at 50 °C under a laminar flow hood. Analyses were carried out in triplicate and each sample was measured for 1000 s. To check the accuracy of the method, a standard As solution of known concentration was measured (Certipur® Arsenic ICP Standard, Merck KGaA, Germany) with a recovery of 99 ± 1%.

μXRF and FE-SEM-EDX analyses

Micro X-ray fluorescence (μXRF) and field emission-scanning electron microscopy-energy dispersive X-ray (FE-SEM-EDX) analyses were performed on soil thin sections. Thin sections were prepared by embedding 20 g of soil in epoxy resin (L.R. White Resin, Polyscience Europe GmbH, Germany) and using a solidification catalyst (L.R. White Accelerator, Polyscience Europe GmbH, Germany) at 2 μl/ml ratio. After hardening, the block was cut along the sedimentation axis and glued onto a glass slide. Finally, the thickness was reduced to 32 μm using a diamond abrasive disk.

μXRF analyses were carried out using a M4 Tornado spectrometer (Bruker Nano GmbH, Germany, Berlin). Analyses were conducted with a Rh target (50 kV, 600 μA) and polycapillary optics providing a spot size of 25 μm. X-ray fluorescence signal was collected by two XFlash® silicon drift detectors (FWHM < 140 eV at the Mn Kα) with an active area of 30 mm^2 placed at 45° to X-ray beam. Analyses were carried out under vacuum (20 mbar), using a sampling step of 20 μm and 10 ms dwell time. X-ray fluorescence hyperspectral data were processed using PyMca 5.1.3 (Solé et al. 2007) and Datamuncher (Alfeld and Janssens 2015) software. A FE-SEM Zeiss Σigma 300 VP (Zeiss Oberkochen, Germany) working at 15 kV and equipped with an energy dispersive spectrometer (EDX) C-Max^N SDD with an active area of 20 mm^2 (Oxford Instruments, Oxford, United Kingdom) was used to study the element distribution at the (sub)micrometric scale.

Results and discussion

Physico-chemical and mineralogical characterization of the soils

Physical and chemical properties of the soil and mine tailing samples are reported in Table 1. All the samples had a pH ranging from 3.6 to 4.3 and a sandy loam texture, with a sand fraction between 56.0 and 65.7%, silt between 24.9 and 33.3%, and a clay fraction of 9.4–15.0%. The organic matter (OM) content was higher in S1 (10.9%) and quite low in S4 (2.5%).

All the samples showed a similar concentration of major elements (expressed as oxides) except for Fe_2O_3 and SO_3, which were much higher in S4 and S3. The As concentration in the three soils increased from S1 (145 mg/kg) to S3 (13,300 mg/kg) and reached values of 40,200 mg/kg in the mine tailing (S4). All the values strongly exceed the Italian legislation limit for As in soil, which is set at 20 mg/kg (Decree of the Italian Ministry Council 2006). The higher the distance from the dismissed plant, the lower the As concentration. The mine tailing, showing the highest As concentration, was collected next to the treatment plant. The As concentration was lower in S2 and S3, which were collected at a distance of 33 and 45 m from the plant, respectively. Finally, S1, which was collected on the other side of the creek (at a distance of 130 m from the plant) showed an As concentration much lower than S2 and S3. Both Fe_2O_3 and SO_3 increased from S1 to S4 together with As concentration (Table 1).

The mineralogy of the samples was characterized by the presence of silicates and aluminosilicates such as quartz, microcline, albite, illite/muscovite, and kaolinite (Fig. 2).

Vermiculite was clearly visible in S2 diffractogram and weakly present in S1, while a weak signal relative to the 100% diffraction peak of sepiolite was observed in S2. Moreover, in sample S4, the weak reflections at $d = 3.11$, 3.08, 5.09, 5.74, and 5.94 Å were attributed to Jarosite ($KFe_3(SO_4)_2(OH)_6$) (Warshaw 1956), a mineral which is usually formed from the oxidation of pyrite (or arsenopyrite) in the presence of K in very acid environments (Fanning et al. 2002; Kim et al. 2014; Savage et al. 2000). No primary As-bearing minerals (e.g., arsenopyrite, orpiment, realgar) or secondary phases (e.g., Fe arsenates and sulphoarsenates) were detected by XRPD. Two small peaks at $d = 2.54$ and 1.51 Å could be attributed to scarcely ordered Fe oxides/hydroxides, likely ferrhydrite ($Fe_5HO_8 \cdot 4H_2O$) or shwertmannite ($Fe_8O_8(OH)_6SO_4$). However, a final identification of these phases could not be made since the main peaks were barely visible and the weaker reflections were not detectable. Despite the presence of Fe oxides/hydroxides and/or hydrosulfates was not clearly confirmed by XRPD, microscopic analyses suggested their presence in soils and tailing in high amounts (see "As distribution in the soils"), most probably as poorly

Table 1 Arsenic and major elements concentration of the soil (S1–S3) and tailing (S4) samples. Some physical and chemical properties are also reported

Sample	As (mg/kg)	SiO_2 (%)	Al_2O_3 (%)	Na_2O (%)	MgO (%)	K_2O (%)	CaO (%)	TiO_2 (%)	Mn_2O (%)	Fe_2O_3 (%)	SO_3 (%)	P_2O_5 (%)	pH (H_2O)	TOC (%)	Sand (%)	Silt (%)	Clay (%)
S1	145	66.17	12.95	4.53	1.09	2.08	0.50	0.45	0.02	3.10	0.26	0.15	4.3	10.9	59.6	25.4	15.0
S2	4640	63.28	13.50	3.36	1.00	4.08	0.59	0.32	0.04	3.86	0.26	0.15	3.7	5.4	59.9	28.3	11.9
S3	13,300	52.23	12.16	1.93	0.52	5.12	0.50	0.35	0.03	6.37	0.65	0.26	4.3	4.7	65.7	24.9	9.4
S4	40,200	53.62	9.51	2.23	0.29	3.69	0.41	0.31	0.02	9.61	1.59	0.22	3.6	2.5	56.0	33.3	10.7

ordered phases. Their crystallization from amorphous Fe oxides/hydroxides could have been hindered by the high sulphate concentration (Langmuir et al. 1999).

The absence of both arsenopyrite and pyrite, the occurrence of poorly crystalline to amorphous Fe oxides/hydroxides and small amount of jarosite suggested a high degree of weathering of these samples, which certainly occurred under oxidizing conditions.

As distribution in the soils

μXRF chemical maps (Fig. 3) showed that the As signal increased moving from S1 to S4 and the same was observed for Fe and S. All these three elements were generally found in the same areas, except for some spots in which only the co-presence of As and Fe was observed. Moreover, it can be noticed that As and Fe form aggregates around silicates or aluminosilicates (Si map). Correlations between Fe and As are clearly visible in Fig. 4a. The scatterplot (obtained by plotting the K-line fluorescence signals of As and Fe) shows that three different As/Fe ratios could be identified. Excluding the blue group, which represents Fe-rich domains, the largest part of the scatter points belongs to As/Fe ratios comprised within the red lines (Fig. 4a). The sample areas where these As/Fe ratios are distributed are represented in red in Fig. 4b. Moving from S1 (low As concentration) to S4 (high As concentration), the red areas increased at the expenses of Fe-rich components (blue areas). Only few scatter points (bordered with green lines) showed a higher As/Fe ratio (Fig. 4a). However, the sample areas characterized by this As/Fe ratio were very small (< 100 μm) and were detected only in S3 and S4 (Fig. 4c). At a higher resolution, FE-SEM-EDX analyses (Fig. 5) showed that the sample areas possessing an intermediate As/Fe ratio (red areas of Fig. 4) were mainly soil aggregates with a variable composition. Iron was the major element followed by As. However, in some cases, S was also detected. This variable composition could explain the high points dispersion within the red group (Fig. 4a). As an example, Fig. 5a revealed that darker gray regions, characterized by the presence of Fe and As, are covered by brighter particles rich in Fe and S but with a substantially reduced As signal (Fig. 5b, d). However, these objects did not show a fixed chemical composition and therefore their nature could not be clearly identified. XRPD did not reveal any As/Fe mineral but, from SEP data (Table 2), this variable composition could be attributed to the adsorption of As on amorphous and/or scarcely ordered Fe oxides/hydroxides, as described in "Prediction of As mobility". On the contrary, FE-SEM-EDX analyses on the green areas of Fig. 4 evidenced the presence of very few "bright" minerals of 20–50 μm whose composition was fixed and characterized by the presence of As and Fe (Fig. 6a). Semi-quantitative EDX analysis of these minerals (Fig. 6b) suggested that it is a Fe arsenate, most probably scorodite, not detected by XRPD. Iron arsenates could form at pH < 3

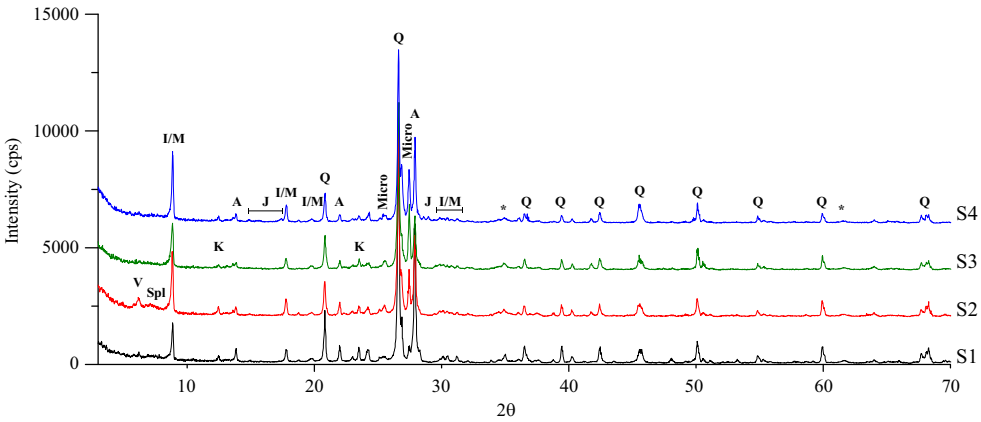

Fig. 2 X-ray diffraction patterns of soils and mine tailing from "Crocette" gold mine. Letters and symbols refer to illite/muscovite (I/M), kaolinite (K), quartz (Q), microcline (Micro), albite (A), vermiculite (V), sepiolite (Spl), jarosite (J), and Fe-oxides/hydroxides (*)

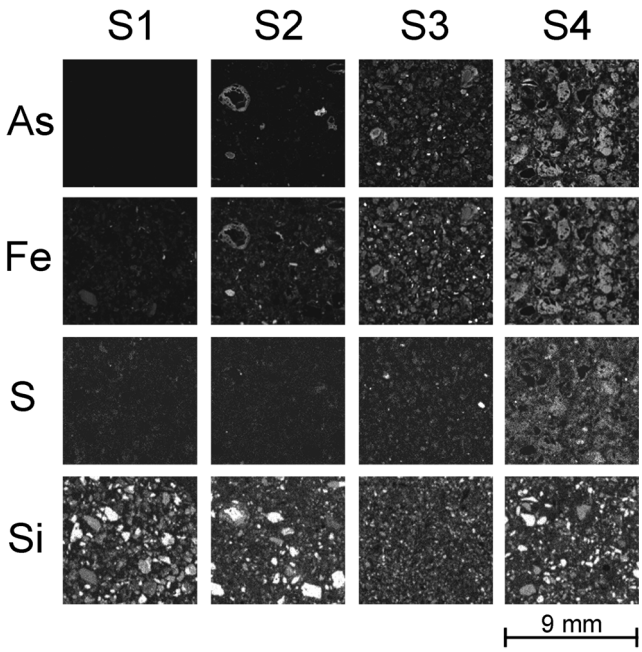

Fig. 3 μXRF As, Fe, S, and Si distribution maps in the thin sections prepared from the four samples. Brighter areas correspond to higher concentrations

(Langmuir et al. 2006), and the kinetics of formation increase as pH decreases (Paktunc et al. 2008). In the case of the soils and mine tailing form "Crocette," the pH ranged between 3.6 and 4.3 (Table 1). Therefore, the presence of these small amounts of Fe arsenates could be attributed to the first stage of Fe/As sulfide oxidation. The pH of the site should allow the formation of Fe oxides/hydroxides (which require a pH > 3 and oxidative conditions) after the weathering of pyrite and arsenopyrite, hindering the crystallization of jarosite which, in fact, is weakly present only in S4 (it requires a pH < 3.5 for formation) (Fanning et al. 2002).

In order to identify other As-bearing phases, Fe/S and As/S scatterplots were also studied (Fig. 7a and b, respectively). Both scatterplots showed three clear ratios and a noisy region. Fe/S scatterplot (Fig. 7a) is characterized by a Fe-rich group (green), an S-rich group (blue), and a region where both elements are detected (red). FE-SEM-EDX analyses on the green areas (Fig. 7c) showed the presence of iron minerals containing As with a Fe/As weight ratio ranging from 3.2 to 3.5. Sulfur was found in very low concentrations (< 1.5%). All the scatter points within the green lines in Fig. 7a are also enclosed by the yellow lines (As-rich domains) in Fig. 7b. Analyzing the points within the red group in Fig. 7a, three different types of minerals were identified (Fig. 7d–f). FE-SEM-EDX analyses suggested the presence of jarosite (Fig. 7d), iron sulfides (most likely greigite, Fe_3S_4) (Fig. 7e), and probably sulphoarsenates (Fig. 7f). The particle

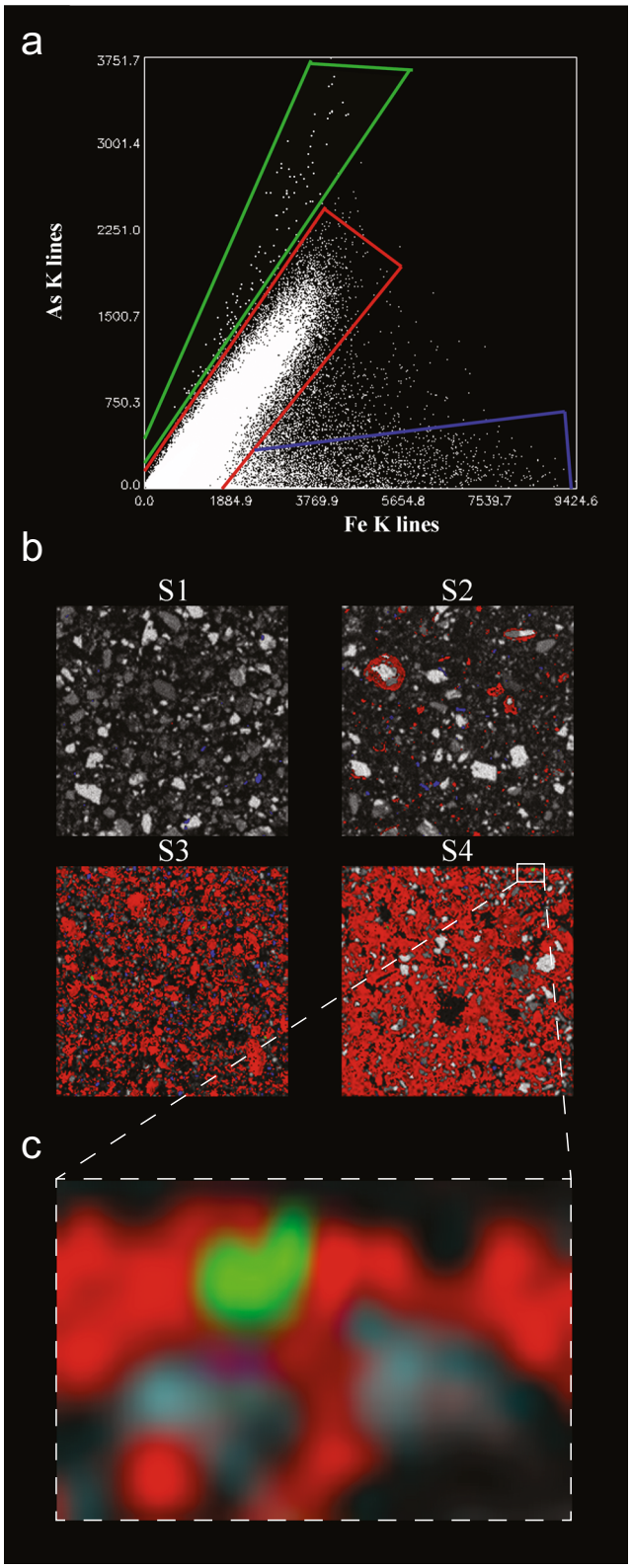

Fig. 4 **a** As vs. Fe scatterplot obtained using fluorescent K-line signals. Three different As/Fe ratios are visible: iron-rich regions (blue group), medium As/Fe ratio regions (red group), and high As/Fe ratio regions (green group). **b** Areas on the sample (blue, red, and green) in which the three As/Fe ratios were measured. Si map (gray scale) was used as background (map size 1 × 1 cm). **c** S4 map magnification evidencing an area with an As/Fe ratio belonging to the green group

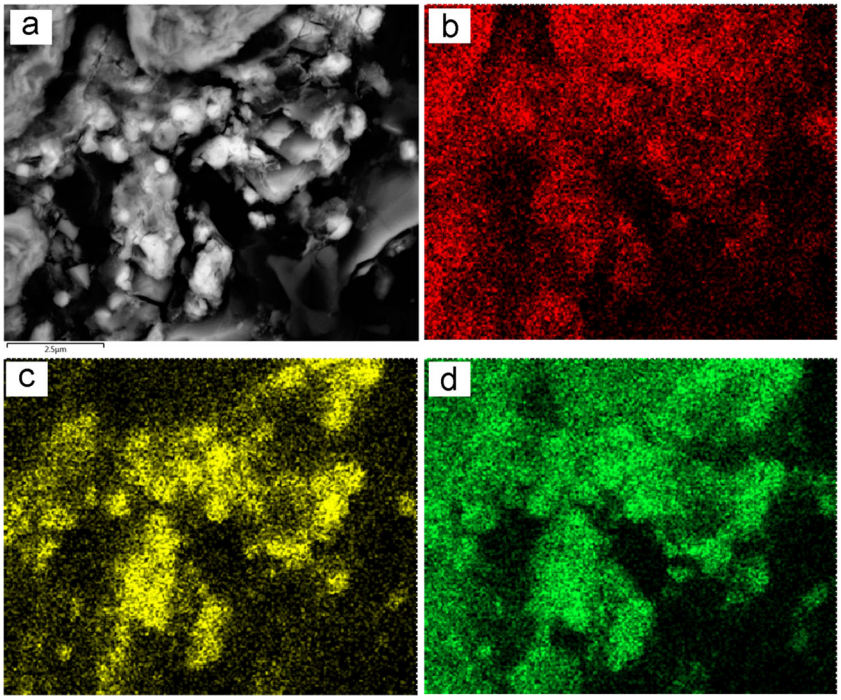

Fig. 5 **a** Backscattered electron image and chemical maps of **b** As, **c** S, and **d** Fe of an area characterized by an As/Fe ratio belonging to the red group of Fig. 3. As and Fe show the same distribution while As and S are uncorrelated

presented in Fig. 7f showed an As/S ratio belonging to the pink group (Fig. 7b). Backscattered micrographs (Fig. 7f) showed that the fluorescence signal comes from the bright part of these grains, which keeps together the quartz particles (dark gray) and which are characterized by the presence of As, Fe, S, as well as a small concentration of Si and Al.

Finally, some points in the database belong to the blue group in Fig. 7a and to the turquoise group in Fig. 7b. FE-SEM-EDX analyses (data not shown) reveal that they could be charcoal residues.

Prediction of as mobility

Important information on the potential mobility of As can be derived from SEP data (Table 2). Each fraction extracted by SEP can be attributed to a particular chemical fraction of As which is bound (or adsorbed) to a specific soil component, and the strength of the As interaction with the soil phases increases at higher extraction steps.

Except for S1, more than 90% of the total As in S2, S3, and S4 samples was extracted in the first three steps. The exchangeable As fraction (step 1), corresponding to soluble As forms, was very limited: 0.6, 0.2 and 0.3% in S2, S3, and S4, respectively. These values correspond to 27 mg of As/kg of soil for S2 and S3 and 120 mg/kg of soil for S4.

The amount of As specifically adsorbed to soil particles (step 2) ranged from 7.6 to 25.2% of the total As, which means that 1–3 g of As/kg of soil could be mobilized by phosphates. Minerals such as kaolinite, smectite, illite, and non-crystalline Al hydroxides have a greater affinity for phosphate adsorption than arsenate. Moreover, the pH of the samples (3.6–4.3) is more likely to promote the adsorption of phosphate rather than arsenate on these mineral phases (Violante and Pigna 2002). According to Violante and Pigna (2002), starting with a molar ratio $AsO_4/PO_4 = 1$, in the presence of kaolinite, smectite, illite, and non-crystalline Al hydroxides, the ratio of sorbed

Table 2 Amount of As (% of total As) extracted after each step of the sequential extraction procedure

Extraction step	Description	S1 % of total As	S2	S3	S4
1	Non-specifically sorbed	2.2 ± 0.2	0.6 ± 0.2	0.2 ± 0.1	0.3 ± 0.1
2	Specifically sorbed	10.7 ± 2.1	25.2 ± 2.7	11.9 ± 2.3	7.6 ± 3.9
3	Associated to amorphous Fe oxides/hydroxides	49.8 ± 0.8	67.2 ± 2.9	85.5 ± 1.5	87.1 ± 4.8
4	Associated to well crystalline Fe oxides/hydroxides	27.9 ± 1.1	1.6 ± 0.3	1.4 ± 0.8	4.7 ± 1.2
5	Residual	9.4 ± 1.2	5.4 ± 1.1	1.0 ± 0.6	0.3 ± 0.2

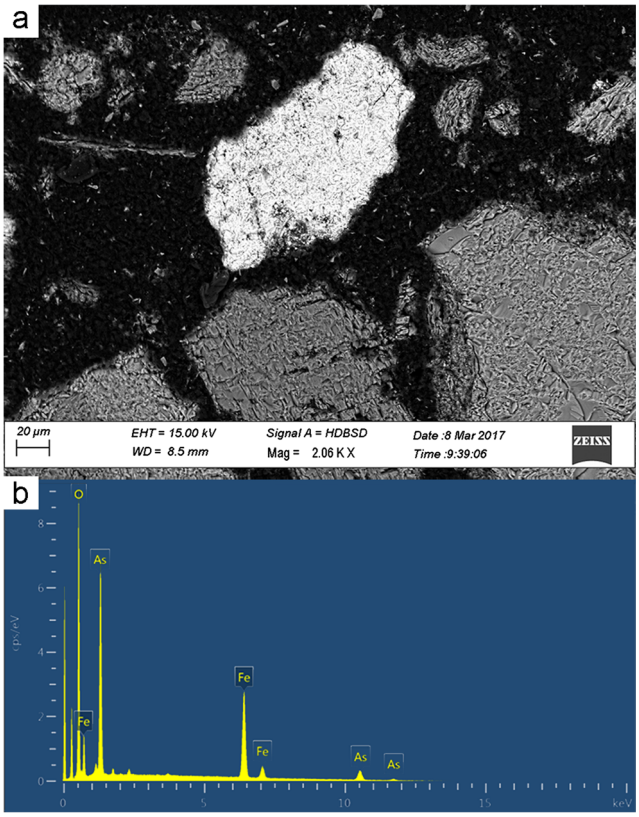

Fig. 6 **a** Backscattered electron image of an area characterized by the As/Fe ratio of the green group of Fig. 4. **b** EDX analysis shows that the brighter particle is Fe arsenate

AsO_4/sorbed PO_4 could range between 0.2 and 0.5. However, by considering the very high AsO_4/PO_4 molar ratio (Table 1), only a small part of the As extracted in this step can be mobilized by phosphate competition.

As mentioned in the previous section, the As bound to amorphous Fe oxides/hydroxides (step 3) is the most represented fraction and is likely to be scarcely mobile, especially in such oxidizing environment. In fact, a number of As immobilization strategies exploit amorphous Fe oxides/hydroxides to reduce the risks associated with As pollution (Nazari et al. 2017). Moreover, amorphous Fe oxides/hydroxides are stable in a wide pH range, which make them more appropriate for As stabilization than other minerals, like scorodite (Nazari et al. 2017). The mobility of the As bound to Fe oxides/hydroxides depends on the pH and redox potential and could be increased either by As desorption from these phases or the dissolution of Fe oxides/hydroxides. In the first case, As desorption from Fe oxides/hydroxides is usually observed under oxidizing conditions at pH > 8 (Lumsdone et al. 2001). Only when the concentration of Fe hydroxides is lower than 1%, the As desorption can occur at a lower pH (about 6) (Lumsdone et al. 2001). However, all the studied samples are characterized by a low pH (about 4) and oxidizing conditions, and therefore the As extracted in this step can be considered non-mobile. Under the studied oxidizing conditions, the most stable As form is $H_2AsO_4^-$ (Smedley and Kinninburgh 2002). However, in the case of alterations of the redox environment from oxidizing to reducing conditions, the reductive dissolution of Fe oxides/hydroxides would promote the release of As into solution (Smedley and Kinninburgh 2002). The process would be additionally favored by the concurrent reduction of arsenate to arsenite, which is scarcely retained by clay minerals and Al oxides (Martin et al. 2014). By taking into account the alternating oxic (spring-summer seasons) and anoxic (prolonged period of snow covering) conditions of the soils under the studied environment, it is possible to hypothesize a potentially long-term high mobility of As due to the above-mentioned processes of Fe oxides/hydroxides dissolution during the winter season (Jeong et al. 2015).

Another factor which may affect the stability of Fe oxides/hydroxides is the reducing action of soil organic matter. Soluble organic matter can also cause the dissolution of Fe oxides/hydroxides by Fe complexation (Lindsay 1991). Moreover, organic matter can compete with As for the sorption sites on Fe oxides/hydroxides (Bauer and Blodau 2006). This aspect should be taken into consideration in particular for sample S1, where TOC exceeds 10%.

Therefore, the As extracted during the third step should be considered potentially bioavailable, since amorphous Fe oxides/hydroxides are considered non-stable phases (Kim et al. 2014; Niazi et al. 2011). However, the potential bioavailability of this As fraction is not only a consequence of its solubility, but it could be exacerbated by the physiological strategies adopted by certain plants and microorganisms to mobilize Fe from soil. This is observed for example with plants coping with iron deficiency that excrete protons and low molecular weight organic compounds to promote iron mobilization by solubilizing in particular Fe amorphous phases, thus increasing, among others, As availability (Mimmo et al. 2014; Terzano et al. 2015).

The As extracted in steps 4 and 5 was important only in sample S1 where it represented the 27.9 and 9.4% of the total As, respectively. However, the As associated to these two steps can be considered very stable, being sorbed to crystalline phases (e.g., well-crystallized Fe oxides/hydroxides, step 4) or included in their lattice structure (step 5).

Conclusions

In this study, a combination of different laboratory X-ray-based analytical techniques (WDXRF, EDXRF, TXRF, XRD, μXRF), FE-SEM-EDX and a five-step SEP were used to study As-polluted soils and tailings. In particular, samples from the abandoned gold mining site of Crocette (Italy) were investigated as a case study.

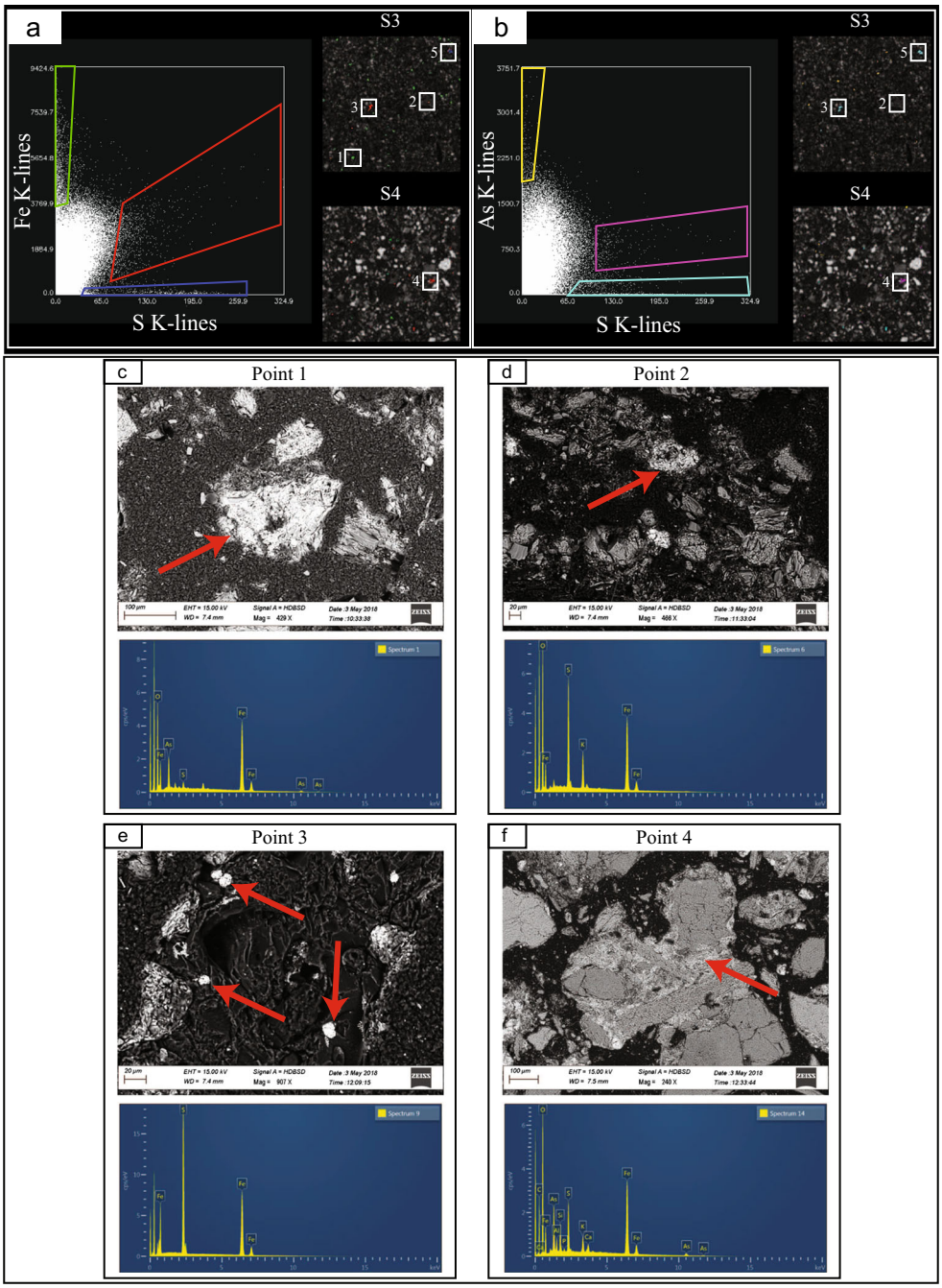

Fig. 7 **a** Fe vs. S and **b** As vs. S scatterplots obtained by using fluorescent K-line signals. The areas in which the different elemental ratios were measured on S3 and S4 thin sections are also shown (small squares) on Si maps (gray scale; map size 1 × 1 cm). Five points with different Fe/S and As/S ratio were identified and analyzed by FE-SEM-EDX and the backscattered images and EDX spectra of **c** point 1, **d** point 2, **e** point 3, and **f** point 4 are reported

The combined approach allowed to get a detailed information about As distribution and mobility in this site; data otherwises not obtainable with conventional analytical methods.

Specifically, a strong weathering of the As-bearing minerals in the topsoil under oxidizing and acidic conditions was observed, as evidenced by the absence of pyrite and arsenopyrite together with the occurrence of amorphous Fe oxides/hydroxides and small amount of jarosite (in the mine tailing).

No As-bearing mineral was detected by XRPD. However, the combination of μXRF hyperspectral data analysis and FE-SEM-EDX allowed to identify small domains of Fe arsenates. In addition, by combining X-ray and micro-analytical data with SEP, additional information about As interaction with soil components was obtained. Arsenic was found mainly associated with poorly ordered Fe oxides/hydroxides, which are known to limit the risk of As leaching and metalloid bioavailability (as evidenced by the growth of a plant coverage on the site despite of the very high As concentrations). However, an important amount of As was still potentially mobilizable (1–3 g of As/kg of soil) and should

therefore be considered in environmental risk analyses and to foresee appropriate remediation actions.

The paper is an example of a study that could be applied to different metal and metalloids in highly contaminated soils relying only on X-ray laboratory equipment and simple chemical extractions.

Acknowledgments All analyses were performed at the "Micro X-ray Lab" of the University of Bari. Dr. S. Stanchi is gratefully acknowledged for the pedologic advice. Finally, we would like to thank two anonymous reviewers for their suggestions.

Funding information The present work is part of a project founded by Ministero dell'Istruzione, dell'Università e della Ricerca—Programmi di Ricerca Scientifica di Rilevante Interesse Nazionale Anno 2010–2011—"Salubrità degli agroecosistemi: processi chimici, biochimici e biologici che regolano la mobilità dell'As nei comparti suolo-acqua-pianta." All analyses were supported by Regione Puglia (Programma Operativo Regione Puglia—FERS 2000–2006—Risorse Liberate—Obiettivo Convergenza).

References

Alfeld M, Janssens K (2015) Strategies for processing mega-pixel X-ray fluorescence hyperspectral data: a case study on a version of Caravaggio's painting supper at Emmaus. J Anal Atom Spectrom 30:777–789. https://doi.org/10.1039/c4ja00387j

Allegretta I, Porfido C, Panzarino O, Fontanella MC, Beone GM, Spagnuolo M, Terzano R (2017) Determination of As concentration in earthworm coelomic fluid extracts by total-reflection X-ray fluorescence spectrometry. Spectrochim Acta B 130:21–25. https://doi.org/10.1016/j.sab.2017.02.003

Arčon I, van Elteren JT, Glass HJ, Kodre A, Šlejkovec Z (2005) EXAFS and XANES study of arsenic in contaminated soil. X-Ray Spectrom 34:435–438. https://doi.org/10.1002/xrs.857

Bauer M, Blodau C (2006) Mobilization of arsenic by dissolved organic matter from iron oxides, soils and sediments. Sci Total Environ 354: 179–190. https://doi.org/10.1016/j.scitotenv.2005.01.027

Caviglia C, Destefanis E, Masciocco L, Re D (2015) Environmental problems related to the presence of arsenic in the Anza valley (Piedmont, north-western Italy). In: Lollino G, Arattano M, Rinaldi M, Giustolisi O, Merechal JC, Grant GE (ed) Engineering Geology for Society and Territory - Volume 3, Springer Cham Heildelberg New York Dprdrecht London, p 421–424

Costantini E, Dazzi C (2013) The soils of Italy. Springer, Dordrecht

Decree of the Italian Ministry Council (2006) Norme in Materia Ambientale, Gazzetta Ufficiale, 88:13–424

Drahota P, Filippi M (2009) Secondary arsenic minerals in the environment: a review. Environ Int 35:1243–1255. https://doi.org/10.1016/j.envint.2009.07.004

Drahota P, Rohovec J, Filippi M, Mihaljevič M, Pychlovský P, Červený V, Pertold Z (2009) Mineralogical and geochemical controls of arsenic speciation and mobility under different redox conditions in soil, sediment and water at the Mokrsko-West gold deposit, Czech Republic. Sci Total Environ 407:3372–3384. https://doi.org/10.1016/j.scitotenv.2009.01.009

Eisler R (2004) Arsenic hazards to humans, plants and animals from gold mining. Rev Environ Contam Toxicol 180:133–165. https://doi.org/10.1007/0-387-21729-0_3

Fanning DS, Rabenhorst MC, Burch SN, Islam KR, Tangren SA (2002) Sulfides and sulfates. In: Dixon JB, Shulze DG (eds) Soil mineralogy in environmental application. Soil Science Society of America Inc., Madison, pp 229–260

Fendorf S, Herbel MJ, Tufano KJ, Kocar BD (2008) Biogeochemical processes controlling the cycling of arsenic in soils and sediments. In: Violante A, Huang PM, Gadd GM (eds) Biophysico-chemical processes of heavy metals and metalloids in soil environments. John Wiley & Sons Inc., Hoboken, pp 313–338

Haffert L, Craw D (2008) Mineralogical controls on environmental mobility of arsenic from historic mine processing residues, New Zealand. Appl Geochem 23:1467–1483. https://doi.org/10.1016/j.apgeochem.2007.12.030

Hopenhayn C (2006) Arsenic in drinking water: impact on human health. Elements 2(2):103–107. https://doi.org/10.2113/gselements.2.2.103

Indorante SJ, Hammer RD, Koenig PG, Follmer LR (1990) Particle-size analysis by a modified pipetted procedure. Soil Sci Soc Am J 54: 560–563. https://doi.org/10.2136/sssaj1990.03615995005400020047x

Javed MB, Kachanoski G, Siddique T (2014) Arsenic fractionation and mineralogical characterization of sediments in the Cold Lake area of Alberta, Canada. Sci Total Environ 500–501:181–190. https://doi.org/10.1016/j.scitotenv.2014.08.083

Jeong D, Kim K, Min DW, Wonyong C (2015) Freezing-enhanced dissolution of iron oxides: effects of inorganic acid anions. Environ Sci Technol 49:12816–12822. https://doi.org/10.1021/acs.est.5b04211

Kim EJ, Yoo JC, Baek K (2014) Arsenic speciation and biaccessibility in arsenic-contaminated soils: sequential extraction and mineralogical investigation. Environ Pollut 186:29–35. https://doi.org/10.1016/j.envpol.2013.11.032

Kocourková-Višková E, Loun J, Sracek O, Houzar S, Filip J (2015) Secondary arsenic minerals and arsenic mobility in a historical waste rock pile at Kaňk near Kuntá Hora, Czech Republic. Mineral Petrol 109(1):17–33. https://doi.org/10.1007/s00710-014-0356-0

Langmuir D, Mahone J, MacDonald A, Rowson J (1999) Predicting arsenic concentrations in the porewaters of buried uranium mill tailing. Geochim Cosmochim Acta 63:3379–3394. https://doi.org/10.1016/S0016-7037(99)00259-8

Langmuir D, Mahoney J, Rowson J (2006) Solubility products of amorphous ferric arsenate and crystalline scorodite ($FeAsO_4{\cdot}2H_2O$) and their application to arsenic behavior in buried mine tailings. Geochim Cosmochim Acta 70:2942–2956. https://doi.org/10.1016/j.gca.2006.03.006

Lenoble V, Bouras O, Beluchat V, Serpaud B, Bollinger JC (2002) Arsenic adsorption onto pillared clays and iron oxides. J Colloid Interface Sci 255:52–58. https://doi.org/10.1006/jcis.2002.8646

Lindsay WL (1991) Iron oxide solubilisation by organic matter and its effect on iron availability. Plant Soil 130:27–34. https://doi.org/10.1007/BF00011852

Lloyd JR, Oremland RS (2006) Microbial transformations of arsenic in the environment: from soda lakes to aquifers. Elements 2(2):85–90. https://doi.org/10.2113/gselements.2.2.85

Lu X, Zang X (2005) Environmental geochemistry study of arsenic in Western Hunan mining area, PR China. Environ Geochem Health 27:313–320. https://doi.org/10.1007/s10653-004-5735-8

Lumsdone DG, Meeussen JCL, Paterson E, Garden LM, Anderson P (2001) Use of solid phase characterization and chemical modelling for assessing the behavior of arsenic in contaminated soils. Appl Geochem 16:571–581. https://doi.org/10.1016/S0883-2927(00)00063-9

Mandal KB, Suzuki KT (2002) Arsenic round the world: a review. Talanta 58:201–235. https://doi.org/10.1016/S0039-9140(02)00268-0

Marabottini R, Stazi SR, Rapp R, Grego S, Moscatelli MC (2013) Mobility and distribution of arsenic in contaminated mine soils and its effects on the microbial pool. Ecotoxicol Environ Saf 96: 147–153. https://doi.org/10.1016/j.ecoenv.2013.06.016

Martin M, Violante A, Ajmone-Marsan F, Barberis E (2014) Surface interactions of arsenite and arsenate on soil colloids. Soil Sci Soc Am J 78:157–170. https://doi.org/10.2136/sssaj2013.04.0133

Masscheleyn PH, Delaune RD, Patrick WH (1991) Effect of redox potential and pH on arsenic speciation and solubility in a contaminated soil. Environ Sci Technol 25:1414–1419. https://doi.org/10.1021/es00020a008

Mimmo T, Del Buono D, Terzano R, Tomasi N, Vigani G, Crecchio C, Pinton R, Zocchi G, Cesco S (2014) Rhizospheric organic compounds in the soil-microorganism-plant system: their role in iron availability. Eur J Soil Sci 65:629–642. https://doi.org/10.1111/ejss.12158

Morin G, Calas G (2006) Arsenic in soils, mine tailings and former industrial sites. Elements 2(2):103–107. https://doi.org/10.2113/gselements.2.2.97

Nazari AM, Radzinski R, Ghahreman A (2017) Review of arsenic metallurgy: treatment of arsenical minerals and the immobilization of arsenic. Hydrometallurgy 174:258–281. https://doi.org/10.1016/j.hydromet.2016.10.011

Niazi NK, Singh B, Shah P (2011) Arsenic speciation ona phytoavailability in contaminated soils using a sequential extraction procedure and XANES spectroscopy. Environ Sci Technol 45:7135–7142. https://doi.org/10.1021/es201677z

Paktunc D, Dutrizac J, Gertsman V (2008) Syntesys and phase transformations involving scorodite, ferric arsenate and arsenical ferrihydrite: implications for arsenic mobility. Geochim Cosmochim Acta 72:2649–2672. https://doi.org/10.1016/j.gca.2008.03.012

Parson C, Margui Grabulosa E, Pili E, Floor GH, Roman-Ross G, Charlet L (2013) Quantification of trace arsenic in soils by field-portable X-ray fluorescence spectrometry: considerations for sample preparation and measurement conditions. J Hazard Mater 262:1213–1222. https://doi.org/10.1016/j.jhazmat.2012.07.001

Porfido C, Allegretta I, Panzarino O, Terzano R, de Lillo E, Spagnuolo M (2016) Bioavailability of arsenic in two Italian industrial contaminated soils. In: Bhattacharya P, Vahter M, Jarsjö J, Kumpiene J, Ahmad A, Sparrenbom C, Jacks G, Donselaar ME, Bundshuh J, Naidu R (eds) Arsenic research and global sustainability: proceedings of the 6th international congress on arsenic in the environment (As2016). CRC Press, London, pp 342–343

Radu T, Diamond D (2009) Comparison of soil pollution concentrations determined using AAS and portable XRF techniques. J Hazard Mater 171:1168–1171. https://doi.org/10.1016/j.jhazmat.2009.06.062

Savage KS, Tingle TN, O'Day PA, Waychunas GA, Bird DK (2000) Arsenic speciation in pyrite and secondary weathering phases, Mother Lode Gold District, Tuolumne County, California. Appl Geochem 15:1219–1244. https://doi.org/10.1016/S0883-2927(99)00115-8

Smedley PL, Kinninburgh DG (2002) A review of the source, behavior and distribution of arsenic in natural waters. Appl Geochem 17:517–568. https://doi.org/10.1016/S0883-2927(02)00018-5

Solé VA, Papillon E, Cotte M, Walter P, Susini J (2007) A multiplatform code for the analysis of energy-dispersive X-ray fluorescence spectra. Spectochim Acta B 62:63–68. https://doi.org/10.1016/j.sab.2006.12.002

Sparks DL (1996) Methods of soil analysis, part 3, chemical methods. Soil Science Society of America, American Society of Agronomy, Madison

Stazi SR, Moscatelli MC, Papp R, Crognale S, Grego S, Martin M, Marabottini R (2017) A multi-biological assay approach to assess microbial diversity in arsenic (As) contaminated soils. Geomicrobiol J 34(2):183–192. https://doi.org/10.1080/01490451.2016.1189015

Strawn D, Doner H, Zavarin M, McHugo S (2002) Microscale investigation into geochemistry of arsenic, selenium and iron in soil developed in pyritic shale materials. Geoderma 108:237–257. https://doi.org/10.1016/S0016-7061(02)00133-7

Terzano R, Cuccovillo G, Gattullo CE, Medici L, Tomasi N, Pinton R, Mimmo T, Cesco S (2015) Combined effect of organic acids and flavonoids on the mobilization of major and trace elements from soil. Biol Fertil Soils 51(6):685–695. https://doi.org/10.1007/s00374-015-1009-0

Van der Snickt G, Legrand S, Caen J, Vanmeert F, Alfeld M, Janssens K (2016) Chemical imaging of stained-glass windows by means of macro X-ray fluorescence (MA-XRF) scanning. Microchem J 124:615–622. https://doi.org/10.1016/j.microc.2015.10.010

Vaughan DJ (2006) Arsenic. Elements 2(2):71–75. https://doi.org/10.2113/gselements.2.2.71

Violante A, Pigna M (2002) Competitive sorption of arsenate and phosphate on different clay minerals and soils. Soil Sci Soc Am J 66(6):1788–1796

Warshaw CM (1956) The occurrence of jarosite in underclays. Am Mineral 41(3–4):288–296

Wenzel WW, Kirchbaumer N, Prohaska T, Stingeder G, Lombi E, Adriano DC (2001) Arsenic fractionation in soils using an improved sequential extraction procedure. Anal Chim Acta 436:309–323

World Health Organization (WHO) (2011) Guidelines for drinking-water quality. WHO, Geneve

Zobrist J, Dowdle PP, Davis JA, Oremland RS (2000) Mobilization of arsenite by dissimilatory reduction of adsorbed arsenate. Environ Sci Technol 34:4747–4753. https://doi.org/10.1021/es001068h